Role of Cisplatin in Inducing Acute Kidney Injury and Pyroptosis in Mice via the Exosome miR-122/ELAVL1 Regulatory Axis

Bei ZHU[1], Juan HE[2], Xiaoshuang YE[3], Xiaohua PEI[1], Yun BAI[1], Fei GAO[1], Lulu GUO[1], Henzhu YONG[1], Weihong ZHAO

[1]Department of Geriatric, The First Affiliated Hospital of Nanjing Medical University, Nanjing, Jiangsu, China, [2]Department of Nephrology, Xian NO.1 Hospital, Xi'an, China, [3]Department of Nephrology, Jiangsu Geriatric Hospital, Nanjing, Jiangsu, China.

Received May 5, 2023
Accepted September 20, 2023

Summary

Although cisplatin is an effective chemotherapy drug for the treatment of various cancers, its clinical use is limited due to its side effects, especially nephrotoxicity. Unfortunately, acute kidney injury (AKI) caused by cisplatin remains one of the main challenges in effective cancer treatment. Evidence increasingly suggests that renal inflammation and pyroptotic inflammatory cell death of renal tubular epithelial cells (RTECs) mainly determine the progression and outcome of cisplatin-induced AKI. However, it is not clear how cisplatin regulates the pyroptosis of RTECs cells in AKI. The current study aimed to determine the regulation mechanism of AKI induced by cisplatin. We used cisplatin to induce AKI *in vivo*. We performed H&E staining of mouse kidney tissue sections and evaluated serological indicators of kidney injury (including blood urea nitrogen (BUN), serum creatinine, and tumor necrosis factor-alpha (TNF-α)). We used immunohistochemistry and western blot to detect the important substrate protein gasdermin D (GSDMD) and key target caspase-1 of pyroptosis, respectively. Cisplatin induced mouse AKI and RTECs pyroptosis. HK2 cell-derived exosomes treated with cisplatin influenced pyroptosis of the surrounding HK2 cells. Cisplatin-treated HK2 cells exosome-derived miR-122 regulated pyroptosis in the surrounding cells. Exosome-derived miR-122 affected cisplatin-induced AKI and HK2 cells pyroptosis by regulating the expression of embryonic lethal abnormal vision (ELAVL1). These results suggest that exosome miR-122 inhibited pyroptosis and AKI by targeting ELAVL1 under cisplatin treatment, and this offers a potential target for the treatment of AKI.

Keywords

Acute kidney injury (AKI) • Cisplatin • ELAVL1 1 • miR-122 • Pyroptosis

Corresponding author

Weihong Zhao, Department of Geriatric, The First Affiliated Hospital of Nanjing Medical University, 300 Guangzhou Road, Nanjing 210029, Jiangsu, China. Email: zhaoweihongzwhhm@126.com

Introduction

Cisplatin is a heavy metal compound with wide clinical use in various tumors. It is one of the most extensively used, effective, and valuable adjuvant chemotherapy drugs for treating diverse malignant tumors, including ovarian cancer, cervical cancer, and so on [1]. Regardless of its potential medicinal effects, the nephrotoxicity it causes is one of the main factors limiting its clinical use [2]. It is estimated that approximately one-third of patients treated with cisplatin suffered from renal dysfunction and injury, especially acute kidney injury (AKI), and this has become the key challenge in the use of cisplatin [3]. Unfortunately, currently, there is no effective treatment to prevent cisplatin-induced AKI [4]. Therefore, exploring the regulation mechanism of cisplatin-induced AKI assumes considerable significance.

AKI is characterized by a sudden decrease in renal function, manifested by an increase in serum creatinine ≥ 0.3 mg/dL or a decrease in urine output of 0.5 mL/kg/h, and is closely linked to high morbidity and mortality [5]. The mechanisms of cisplatin-induced AKI are complex, mainly seen as excessive inflammation and programmed cell death of renal tubular epithelial cells (RTECs) [6]. In the kidney, RTECs are the main target of drug-induced nephrotoxicity and are particularly

Fax +420 241 062 164, e-mail: physres@fgu.cas.cz, www.biomed.cas.cz/physiolres

vulnerable to cisplatin injury [7]. Previous studies have also shown that the common histological feature of cisplatin-induced AKI is renal damage caused by renal tubular cell death [8].

Pyroptosis is a new type of proinflammatory programmed cell death regulated by caspases discovered and confirmed in recent years. Its morphological feature is the formation of plasma membrane pores, leading to the secretion of intracellular components and inflammatory cytokines [9]. Early researchers first observed the phenomenon of pyroptosis in several phagocytes, such as macrophages [10]. However, in recent studies, it has been found that pyroptosis can also be triggered in other types of cells, such as RTECs [11]. A growing number of studies have focused on the role of pyroptosis in AKI. Caspase-11-mediated pyroptosis of RTECs promotes acute renal injury induced by sepsis [12]. The tumor necrosis factor-alpha (TNF-α)/high mobility group box protein 1 (HMGB1) inflammation signal axis participates in the progression of AKI disease by regulating pyroptosis [13]. Acetylbritannilactone can alleviate contrast-induced AKI by reducing pyroptosis [14]. Furthermore, increasing evidence indicates that RTECs pyroptosis and renal inflammation are involved in the regulation of cisplatin-induced AKI progression and outcome. For example, the cleavage of gasdermin D (GSDMD) by caspase-11 can promote cisplatin-induced AKI by triggering RTECs pyroptosis [15]. These studies indicate that the pyroptosis of RTECs is a key event in the occurrence and outcome of cisplatin-induced AKI. However, the exact mechanism by which cisplatin induces AKI by promoting pyroptosis is unclear.

Exosomes are microvesicles of multivesicular bodies with diameters ranging from 20 to 200 nm [16]. Exosomes participate in cell-to-cell communication with recipient cells by fusing with receptor cell membranes and delivering biomolecules such as proteins, DNA, mRNAs, and miRNAs [17]. In recent years, the findings of more and more studies have revealed the function of exosomes in the kidney. On the one hand, exosomes can be used as a marker for early diagnosis and treatment of kidney disease [18]. On the other hand, exosomes target effector cells through the paracrine pathway to play a role in kidney pathophysiology [19]. In a previous study, it was found that injured renal tubular epithelial cells activated fibroblasts through exosome miRNAs to promote renal fibrosis [20]. Limb remote ischemic preconditioning induces systemic upregulation of exo-miR-21, exerting anti-inflammatory and anti-apoptotic effects, thereby protecting from sepsis-induced AKI [21]. However, the regulatory mechanism of exosomal miRNAs in cisplatin-induced AKI is unclear.

We first used cisplatin in a mouse model to induce AKI to investigate whether exosomal miRNAs play a role in cisplatin-induced AKI by regulating pyroptosis. Then, we analyzed the expression of GSDMD, a key substrate protein for pyroptosis, in AKI mice using immunohistochemistry (IHC). We also detected the expression of pyroptosis-related proteins caspase-1 and GSDMD-N using Western blot (WB) analysis. We found that pyroptosis occurred when cisplatin induced AKI in mice.

Next, we conducted in vitro studies. We treated HK2 cell line with cisplatin and detected the expression ofcaspase-1 using immunofluorescence (IF). We also measured the expression of GSDMD-N in HK2 cell line using WB. The experimental results were consistent with animal levels. Therefore, we further studied the regulatory mechanism of cisplatin-induced AKI. When we added cisplatin and GW4869 at the same time, the expressions of caspase-1, NLRP3, and GSDMD were significantly downregulated. These results indicate that cisplatin regulated HK2 cell pyroptosis through exosomes. Further, the gain- or loss- of function experiments were done in vitro and in vivo to clarify that cisplatin affects pyroptosis of RTECs through the exosomal miR-122/ELAVL1 regulatory axis in cisplatin-induced AKI.

Materials and methods

Cell lines and culture conditions

HK2 cells (human renal tubular epithelial cells) were purchased from the Chinese Academy of Sciences, Shanghai Institute of Biochemistry and Cell Biology (Shanghai, China). These cells were grown in Dulbecco's modified eagle medium (DMEM) containing 5% fetal bovine serum (FBS) (37°C, 5% CO2). The HK2 cells were treated with or without 20 μM cisplatin for 24 h.

Animal model of AKI

We procured adult male C57BL/6 mice (8−12 weeks of age) from the Model Animal Research Center of Nanjing University, Nanjing, China. All animal procedures were approved by the Institutional Animal Experimental Ethics Committee. We injected 20 mg/kg cisplatin and constructed the Cisplatin-induced AKI mice model as described previously [22]. We injected these mice with 20 mg/kg body weight cisplatin

intraperitoneally and we injected an equal volume of 0.9% saline for the controls. After 72 hours, the mice were euthanized under anesthesia. We collected blood samples and kidney tissues for further study.

Serum Creatinine, BUN, TNF-α and Histology

We used a Beckman creatinine analyzer II (DXC800; Beckman Coulter) to analyze the serum creatinine concentration in the model mice. We measured blood urea nitrogen (BUN) using a BUN Assay Kit (Nanjing, China) as per the manufacturer's instructions. We detected TNF-α levels using the TNF-α Assay Kit (Nanjing, China) following the manufacturer's instructions. We used a 2 μm-thick section for hematoxylin-eosin (H&E) staining to assess renal tubular histological damage.

Immunohistochemistry

We used paraffin-embedded renal tissue sections of AKI mice to detect the expression of GSDMD (ab219800; 1:1000; Abcam, UK), a marker of pyroptosis, using immunohistochemistry (IHC). The specific experimental procedures of IHC have been detailed in previous reports [23].

Immunofluorescence staining

The HK2 cells were placed on glass slides in 6-well plates. After cisplatin treatment for 24h, the cells were fixed in 4% paraformaldehyde, blocked with 2% BSA and incubated with 0.1% Triton X-100. The HK2 cells were incubated with caspase-1 antibody (sc-398715, Santa Cruz Biotechnology, 1:200, USA) at 4°C overnight. The slides were subsequently incubated with secondary antibody (Alexa Fluor 488-labelled). The nuclei were stained using 4',6-diamidino-2-phenylindole (DAPI). The specific experimental procedures of IHC have been detailed in previous reports [24].

RNA extraction and qRT-PCR

We extracted total RNA and conducted the analysis of real-time quantitative reverse transcription polymerase chain reaction (qRT-PCR) as described earlier [1]. We used TRIZOL reagent (Thermofisher, USA) to extract total RNA from cells and tissues. Taqman probes (Applied Biosystems, USA) were used to quantify miRNAs. Briefly, 1 μg of total RNA was transcribed to cDNA using AMV reverse transcriptase (Takara, Japan) and an RT primer (table 1). The reaction conditions were: 16 °C for 30 min, 42 °C for 30 min and 85 °C for 5 min. Real-time PCR was performed using a Taqman PCR kit on an Applied Biosystems 7300 sequence detection system (Applied Biosystems, USA). The reactions were performed in a 96-well plate at 95 °C for 10 min, followed by 40 cycles of 95 °C for 10 sec and 60 °C for 1 min. U6 was used as the internal control.

Table 1. Primers

	FP	**RP**
Caspase-1	**5'-CGGAATTCACCATGGCCGACAAGGTCCTG -3'**	**5'-CTGCACTGCCTGAGGAGCTGGAAAGGAAGAAAGTACTCCTTGAGAGTCT-3'**
NLRP3	**5'-CTCAGCCTTGCGAAGTTTCA-3'**	**5'-ACCGCATACACACTTGGAGA-3'**
GSDMD	5'-CTCAGCCTTGCGAAGTTTCA-3'	5'-ACCGCATACACACTTGGAGA-3'
ELAVL1	5'-CTCAGCCTTGCGAAGTTTCA-3'	5'-ACCGCATACACACTTGGAGA-3'
GAPDH	5'-CTCAGCCTTGCGAAGTTTCA-3'	5'-ACCGCATACACACTTGGAGA-3'
Stem loop primer	5'-GTCGTATCCAGTGCAGGGTCCGAGGTATT-3'	5'-CGCACTGGATACGACACACCC-3'
U6	5'-CTCGCTTCGGCAGCACA-3'	5'-AACGCTTCACGAATTTGCGT -3'

Exosome isolation and labeling

We used exosome-depleted FBS in the following experiments to avoid the impact of exosomes. FBS was depleted of exosomes using ultracentrifugation at 1×106 g at 4 ˚C for 16 h (Beckman Coulter Avanti J-30I, USA). After being incubated for 48−72 h, the culture medium was harvested and exosomes were isolated by ultracentrifugation. Briefly, cell culture medium was sequentially centrifuged at 300 g for 10 min, 2,000 g for 15 min, and 12,000 g for 30 min to remove floating cells and cellular debris. These were then passed through a 0.22-μm filter. The supernatant was further ultracentrifuged at 1×106 g for 2 h at 4 ˚C, washed in phosphate-buffered saline (PBS), and submitted to a second ultracentrifugation under the same conditions. We quantified exosomes using the bicinchoninic acid (BCA) method. We measured exosomal protein using the BCA protein assay kit (Beyotime Biotechnology, Nantong, China). The final exosome pellets were used immediately.

Transmission electron microscope

Exosomes were precipitated and immediately fixed in 2.5% glutaraldehyde at 4 ˚C for the electron microscope observation. After fixation, specimens were processed through dehydration in gradient alcohol, infiltrated in epoxy resin and then embedded. The ultrathin sections were stained with uranyl acetate and lead citrate and were observed under transmission electron microscope (TEM) (JEM- 1010; JEOL, Tokyo, Japan).

NanoSight tracking analysis (NTA)

We analyzed isolated exosomes using Nanosight LM10 system (Nanosight Ltd, Navato, CA) equipped with a blue laser (405 nm). Nanoparticles were illuminated by the laser and their movement under Brownian motion was captured for 60 seconds and we analyzed the recorded video with NanoSight tracking analysis (NTA) using the Nanosight particle tracking software to calculate nanoparticle concentrations and size distribution.

Western blotting analysis

Protein lysates were fractionated on SDS-polyacrylamide gels and transferred to polyvinylidene fluoride (PVDF) membrane and blocked with 5% skimmed milk in Tris-buffered saline with Tween 20. The membranes were incubated with the primary antibodies, including Caspase-1 rabbit monoclonal antibody (ab207802; 1:1000; Abcam, UK), GSDMD-N rabbit monoclonal antibody (ab215203; 1:1000; Abcam, UK), NLRP3 rabbit monoclonal antibody (ab263899; 1:1000; Abcam, UK), GSDMD rabbit monoclonal antibody (ab219800; 1:1000; Abcam, UK). ELAVL1 rabbit monoclonal antibody (ab200342; 1:1000; Abcam, UK). CD63 rabbit monoclonal antibody (ab134045; 1:1000; Abcam, UK). CD9 rabbit monoclonal antibody (ab92726; 1:2000; Abcam, UK). The protein concentration of the supernatant was determined with a BCA protein assay kit (Synthgene, China). GAPDH served as a loading control and protein bands were quantified using Image J Software.

Luciferase reporter assay

pMIR-ELAVL1-3'-UTR-WT as well as pMIR-ELAVL1-3'-UTR-MUT luciferase reporter plasmids were constructed using Synthgene Biotech (Nanjing, China). The sequences that could bind to miR-122 were partly mutated and inserted into the reporter plasmid in order to identify the binding specificity. Details of the implementation method are given in our previous study [25]. Briefly, HK2 cells were seeded in a 24-well plate until reaching 60% confluence. Each well was co-transfected with luciferase reporter plasmids (0.5 μg) and RNA mimics (100 pmol) using Lipofectamine 2000 (Thermofisher, USA) as per the manufacturer's protocol. We measured the luciferase activity after 48 h of transfection using the Dual-Luciferase Reporter Assay (Promega, Shanghai, China) as per the manufacturer's instructions and normalized to Renilla signals.

siRNA preparation and transfection

We accomplished ELAVL1 knockdown by transfecting cells with siRNA. ELAVL1 and control siRNA were synthesized using Synthgene (China). The specific method is described in our previous report [25]. The sequences were as follows: the ELAVL1 sense GAACATGACCCAGGATGAGTT, the ELAVL1 antisense UUUUGAAGAAGAAUCGUUGcc. SiRNA transfection into HK2 cells was carried out using Lipofectamine 2000 (Thermofisher, USA) as per the manufacturer′ s instructions.

Overexpression plasmid construction

Full-length ELAVL1 from the human cDNA library was cloned into a pcDNA3. 1 vector (Invitrogen; Thermo Fisher Scientific, Inc.). The pcDNA3.1 vector alone (empty plasmid) served as a negative control. HK2 cells were transfected with pcDNA3.1/ ELAVL1 vector (100 nM) or pcDNA3.1 (100 nM) using Lipofectamine 2000 (Thermofisher, USA) as per the manufacturer′ s

instructions. Following transfection for 48 h, the cells were collected for subsequent experiments. The sequence of the ELAVL1 overexpressed plasmid is detailed in the supplementary materials.

Statistical analyses

All experiments were repeated thrice. Data were presented as mean ± standard deviation and analyzed using SPSS 18.0 (SPSS, Inc.). We performed one-way analysis of variance (ANOVA) and post hoc Dunnett's T3 test to compare the differences among and between groups, respectively. $P < 0.05$ was considered to indicate a statistically significant difference.

Results

Cisplatin induced mouse AKI and RTECs pyroptosis

Cisplatin-induced AKI is a serious threat to the health of cancer patients and largely restricts its use in chemotherapy [26]. Therefore, studying the pathogenesis of cisplatin-induced AKI is of great significance. First, we constructed a mouse model of AKI induced by cisplatin. We then detected the extent of histopathological damage to the renal cortex in the mice with cisplatin-induced AKI using H&E staining. As shown in Fig. 1A, cisplatin caused moderate renal tubular injury. The kidney section showed obvious focal tubular epithelial cell swelling, dilation and detachment with moderate tubular vacuole. In addition, the levels of blood urea nitrogen (BUN) (Fig. 1B), serum creatinine (Fig. 1C) and TNF-α (Fig. 1D) were significantly increased in the cisplatin-AKI mice model.

Previous researchers found that pyroptosis plays an important role in many inflammatory diseases, such as cisplatin-induced AKI [23]. Therefore, in this study, we further explored how pyroptosis in involved in cisplatin-induced AKI. First, we detected the expression of GSDMD in kidney tissue using IHC analysis. As shown in Fig. 1E, the expression of GSDMD in the model group (cp) was significantly increased when compared with the control group. Then, we detected the expression levels of caspase-1 and GSDMD-N using WB analysis. The variation trend of the results was consistent with GSDMD (Fig. 1F-G). These in vivo experiments preliminarily elucidated the involvement of pyroptosis in cisplatin-induced AKI.

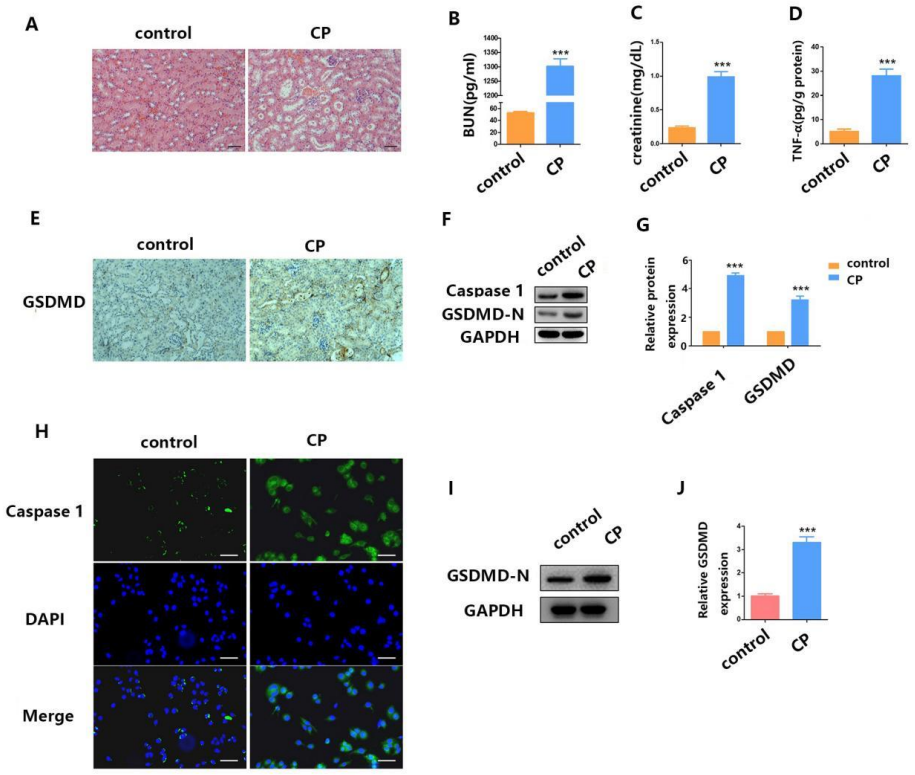

Fig. 1. Cisplatin induces mouse AKI and RTECs pyroptosis. (**A**) H&E staining assays were performed 24 h after surgery in both the cisplatin-induced AKI mouse model group and the control group. (**B-D**) After AKI was induced by cisplatin treatment, we checked the blood for BUN, serum creatinine, and TNF-α concentration. (**E**) The distribution of GSDMD in kidney tissues as measured by IHC. (**F-G**) WB analysis of caspase-1 and GSDMD-N expression in cisplatin-induced AKI mice. (**H**) IF staining shows expression of caspase-1 (green) in cisplatin-treated HK2 cells; Blue fluorescence represents the nucleus (DAPI). Bar, 100 mm. (**I-J**) WB analysis of caspase-1 and GSDMD-N expression in cisplatin-treated HK2 cells. Data are shown as mean ± SEM (n = 3). Asterisks indicate significant differences from the control (*$P < 0.05$; **$P < 0.01$; ***$P < 0.001$).

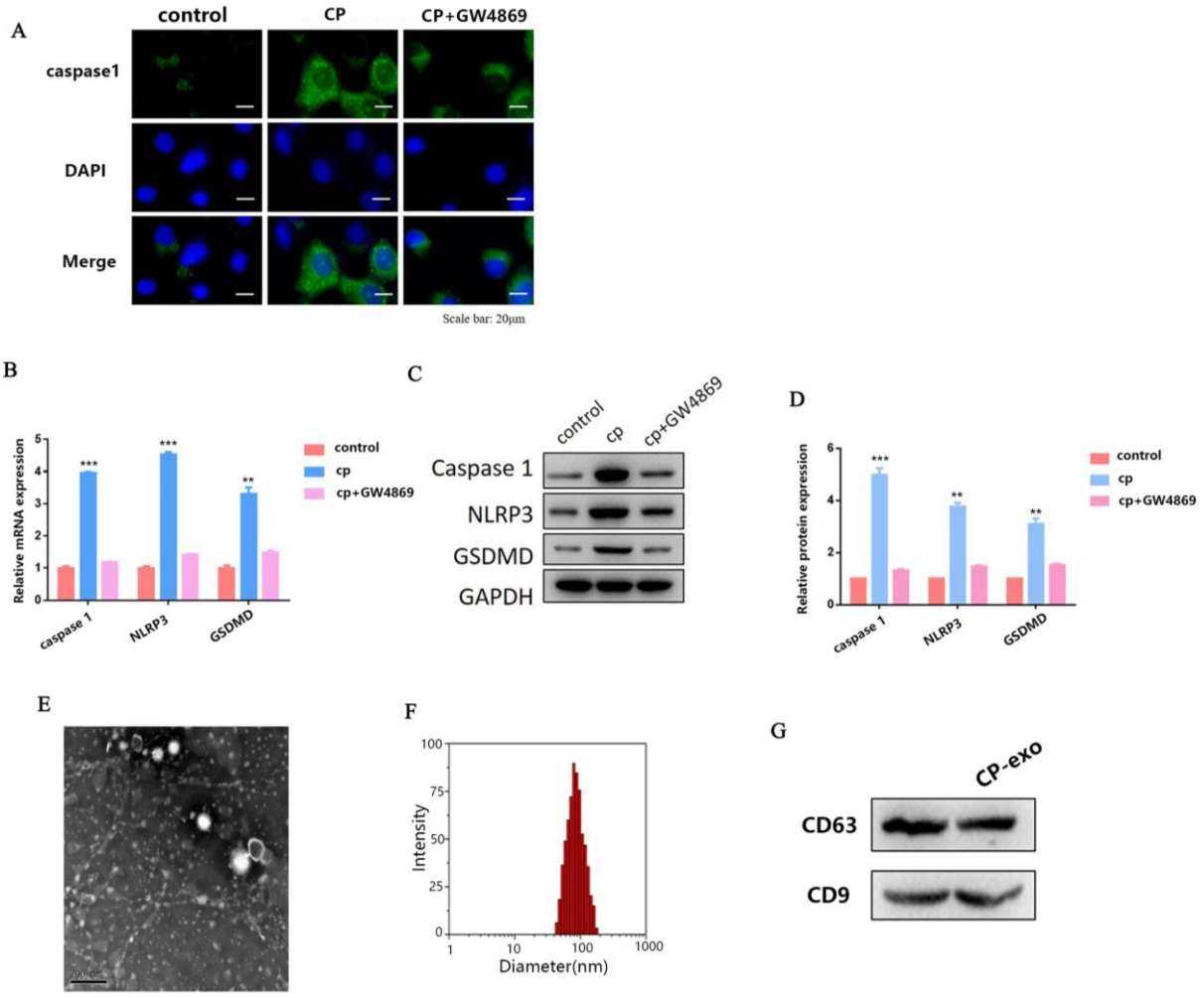

Fig. 2. HK2 cell-derived exosomes treated with cisplatin influence pyroptosis of surrounding HK2 cells. (**A**) IF staining shows expression of caspase-1 (green) in cisplatin-treated and cisplatin+ GW4869-treated HK2 cells, respectively; Blue fluorescence represents the nucleus (DAPI). Bar, 20 mm. (**B**) The qPCR analysis of caspase-1, NLRP3, and GSDMD expression in cisplatin-treated and cisplatin+GW4869-treated HK2 cells. (**C-D**) WB analysis of caspase-1, NLRP3, and GSDMD expression in cisplatin-treated and cisplatin+GW4869-treated HK2 cells. (**E**) The transmission electron microscope (TEM) image of exosomes isolated from HK2 cells, revealing the typical morphology and size (30 and 150 nm). (scale bar, 200 nm). (**F**) The particle diameter (nm) of the population of small vesicles collected from HK2 cells detected using qNano. (**G**) WB shows that exosome marker CD63 and CD9 are expressed in exosomes. Data are shown as mean ± SEM (n = 3). Asterisks indicate significant differences from the control (*P < 0.05; **P < 0.01; ***P < 0.001).

In order to further elucidate the role of pyroptosis in cisplatin-induced AKI, we conducted further studies in vitro. We selected HK2 cell lines (human RTECs) for the study. First, we detected the expression of caspase-1 in HK2 cells using IF when treated with cisplatin. As shown in Fig. 1H, the expression level of caspase-1 in HK2 cells treated with cisplatin was significantly increased when compared with the control group. Then, we detected the expression level of GSDMD-N in HK2 cells when treated with cisplatin. The variation trend of the results was consistent with caspase-1 (Fig. 1I-J). In summary, these in vivo and in vitro results indicate that pyroptosis was involved in cisplatin-induced AKI.

HK2 cell-derived exosomes treated with cisplatin influenced pyroptosis of surrounding HK2 cells.

Previous studies have reported that exosomes play a key role in the development of kidney disease. However, there are only a few reports on cisplatin-induced AKI, and the regulatory mechanism is unclear. Therefore, in the present study, we explored the role of exosomes in cisplatin-induced pyroptosis of HK2 cells. First, we treated HK2 cells with cisplatin and exosome inhibitor GW4869 at the same time, and detected the expression of caspase-1 using IF. As shown in Fig. 2A, the treatment of HK2 cells with cisplatin significantly increased the expression of caspase-1, but after adding GW4869, the expression of caspase-1 was significantly downregulated. This result suggests that exosomes are involved in cisplatin-induced pyroptosis of surrounding HK2 cells.

To further verify our hypothesis, we also detected the mRNA and protein expression levels of caspase-1, NLRP3, and GSDMD using qRT-PCR and WB, respectively. The variation trend of the results was consistent with caspase-1 (Fig. 2B-D). Taken together, these results indicate that exosomes are involved in cisplatin-induced AKI pyroptosis.

Next, we focused on the exosomes in HK2 cells. We further isolated and identified exosomes from HK2 cells. As shown in Fig. 2E, exosomes were characterized using transmission electron microscope (TEM). In the TEM analysis of isolated exosomes, we found round structures with diameters between 30 and 150 nm. We used the qNano analysis to quantify the particle diameter of the population of small vesicles collected from HK2 cells and the mean diameter of HK2-exo was 100 nm (Fig. 2F). We also measured exosome markers CD63 and CD63 in HK2 cells when treated with or without cisplatin. WB assay showed that CD63 and CD63 were all expressed in both ctrl-exo and cp-exo groups (Fig. 2G).

Cisplatin-treated HK2 cells exosome-derived miR-122 regulated pyroptosis in the surrounding cells.

In eukaryotes, miRNAs usually regulate gene expression at the post-transcriptional level. Previous studies have found that abnormal levels of miRNA could be one of the mechanisms explaining dysregulated protein expression in the progression of kidney disease [27]. When evaluating an integrative network of miRNAs and mRNA data, miR-122 was found to be one of the possible master regulators in AKI [28]. Therefore, we speculated that miR-122 was involved in the regulation of cisplatin-induced AKI pyroptosis.

To verify our hypothesis, we first tested the expression of miR-122 in AKI mice and HK2 cells. As shown in Fig. 3A-B, cisplatin treatment significantly reduced miR-122 expression in vivo and in vitro when compared with the control. However, after adding GW4869, the expression of miR-122 significantly increased to reach levels close to the control group (Fig. 3C).

To further explore the role of exosomes derived miR-122 in cisplatin-induced pyroptosis of HK2 cells, we first used the miR-122 mimic and inhibitor to transfect HK2 cells to overexpress (miR-122 OE) and knock down (miR-122 KD) miR-122, respectively. Then, we detected the expression of caspase-1 in surrounding HK2 cells (NC) using IF when adding cisplatin-treated HK2 cell-derived exosomes (cp-exo) and cisplatin-treated miR-122 OE HK2 cell-derived exosomes (cp-exo+miR-122 OE) treatments, separately. As shown in Fig. 3E, the expression level of caspase-1 was significantly increased when compared with the NC group when cp-exo treatment was added. In contrast, the expression level of caspase-1 was significantly decreased when cp-exo+miR-122 OE treatment was added.

We also tested the expression of caspase-1 in miR-122KD HK2 cell line. The results showed that the expression of caspase-1 was also significantly increased in miR-122 KD HK2 cell line when compared with the NC group. Next, we also detected the mRNA and protein expression levels of caspase-1, NLRP3, and GSDMD using qRT-PCR and WB, respectively. The variation trend of the results was consistent with caspase-1 (Fig. 3E-G). The above results further indicate that the miR-122 involved in cisplatin-treated HK2 cell exosomes affected the surrounding HK2 cell pyroptosis.

We further explored the regulatory mechanism of miR-122 involved in the regulation of pyroptosis in cisplatin-treated HK2 cells. First, we detected the expression level of miR-122 using qRT-PCR in NC, NC+cp-exo, NC+cp-exo-miR-122 OE, and NC+miR-122 KD groups. As shown in Fig. 3H, the expression level of miR-122 was significantly decreased when cp-exo treatment was added. In contrast, the expression level of miR-122 was significantly increased when cp-exo+miR-122 OE treatment was added.

We also tested the expression of miR-122 in miR-122KD HK2 cell line. The result was in line with expectations. Then, we predicted the relevant targets. We used the TargetScan Human 7.2 software and found that miR-122 targeted ELAVL1. As shown in Fig. 3I, ELAVL1 gene was found to contain putative sites of the 3'-UTR untranslated region (3'-UTR) that matched to the miR-122 seed region.

To investigate whether miR-122 targets ELAVL1 in cisplatin-induced AKI, we set up the luciferase reporter plasmid (containing the wild-type (WT) and mutation-type (MUT) 3'-UTR) of target gene ELAVL1 using luciferase reporter vector. We further used the transfection reagent to transfect these reporter gene plasmids (WT and MUT) into HK2 cells together with the miR-122 mimic or miR-122 inhibitor, respectively. Compared with control groups, WT reporter activity was predominantly decreased in HK2 cells when transfected with miR-122 mimic. In contrast, WT reporter activity was significantly upregulated in HK2 transfected with miR-122 inhibitor, while the transfection of miR-122 mimic and miR-122 inhibitor did not affect the

activity of MUT reporter activity (Fig. 3J).

Then, we detected the protein expression of ELAVL1 in vivo and in vitro when cisplatin treatment was added. As shown in Fig. 3K-L, the expression level of ELAVL1 was significantly increased when adding cisplatin treatment. To elucidate the role of exosomes in regulating the expression of ELAVL1, we also added GW4869. The results showed that the expression of ELAVL1 was significantly decreased in HK2 cells at the same time when cisplatin and GW4869 were added (Fig. 3M).

Finally, we conducted a rescue experiment. We measured the protein expression of ELAVL1 in NC, NC+cp-exo, NC+cp-exo-miR-122 OE, and NC+miR-122 KD groups. As shown in Fig. 3N, the expression level of ELAVL1 was significantly increased when cp-exo treatment was added. In contrast, the expression level of ELAVL1 was significantly decreased when cp-exo+miR-122 OE treatment was added. We also tested the expression of ELAVL1 in miR-122KD HK2 cell line. The result was in line with expectations. All these results suggest that miR-122 negatively regulated ELAVL1 expression by directly binding to the 3'-UTR region of ELAVL1 in cisplatin-induced AKI.

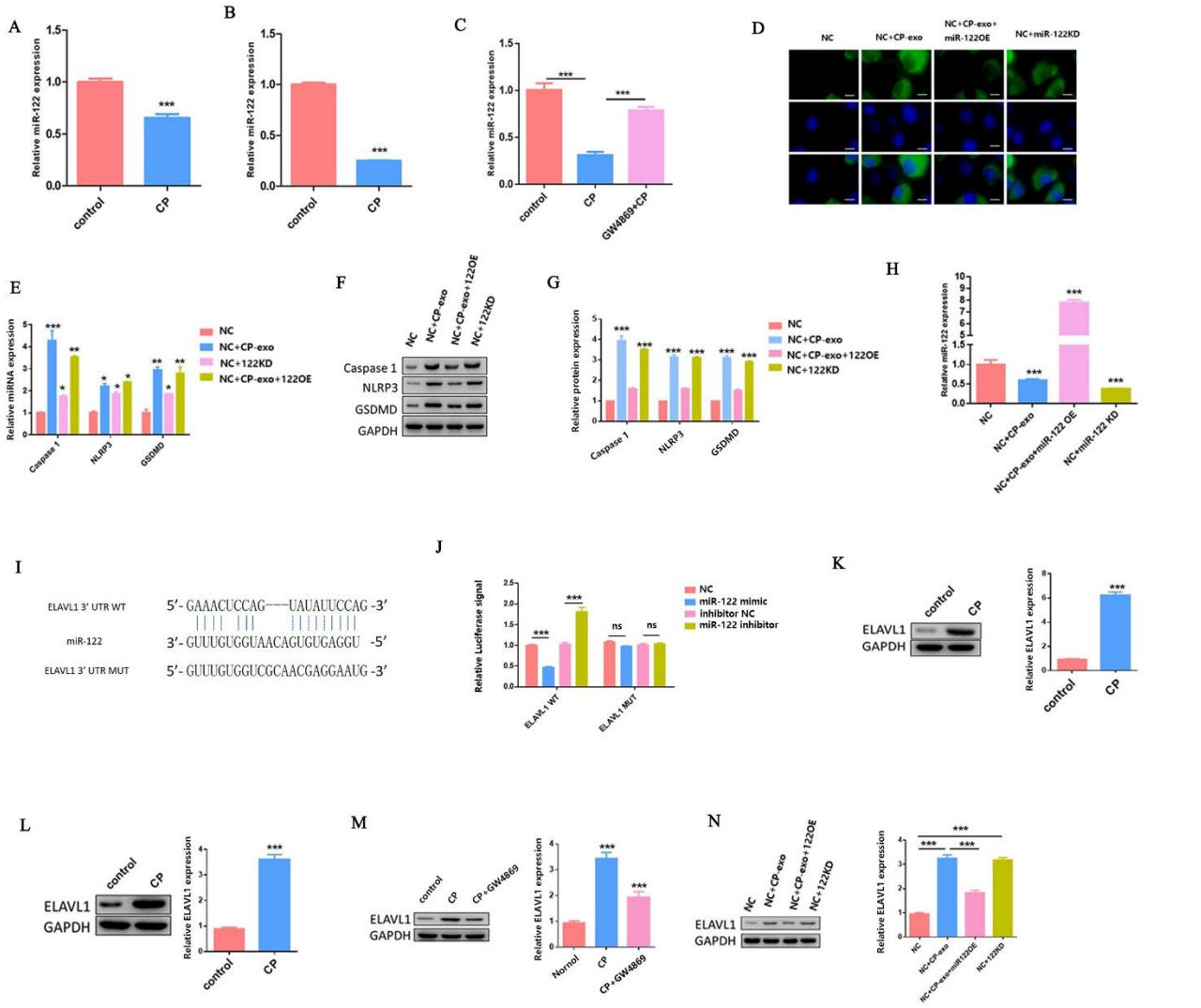

Fig. 3. Cisplatin-treated HK2 cells exosome-derived miR-122 regulates pyroptosis in surrounding cells.
(**A-B**) The qPCR analysis of miR-122 expression in vivo and in vitro when adding cisplatin treatment. (**C**) The qPCR analysis of miR-122 expression. (**D**) IF staining shows expression of caspase-1 (green); Blue fluorescence represents the nucleus (DAPI). Bar, 20 mm. (**E**) The qPCR analysis of caspase-1, NLRP3, and GSDMD expression. (**F-G**) WB analysis of caspase-1, NLRP3, and GSDMD expression. (**H**) The qPCR analysis of miR-122 expression. (**I**) 3'-UTR base pairing diagram of miR-122 and ELAVL1. (**J**) Cells are co-transfected with miR-122 mimics/inhibitor and a luciferase reporter containing a fragment of the ELAVL1 3'-UTR harboring either the miR-122 binding site (ELAVL1-3'-UTR-WT) or a mutant (ELAVL1-3'-UTR-MUT). (**K-N**) The protein expression of ELAVL1 in vivo and in vitro under different processing conditions. Data are shown as mean ± SEM (n=3).Asterisks indicate significant differences from the control (*P < 0.05; **P < 0.01; ***P < 0.001).

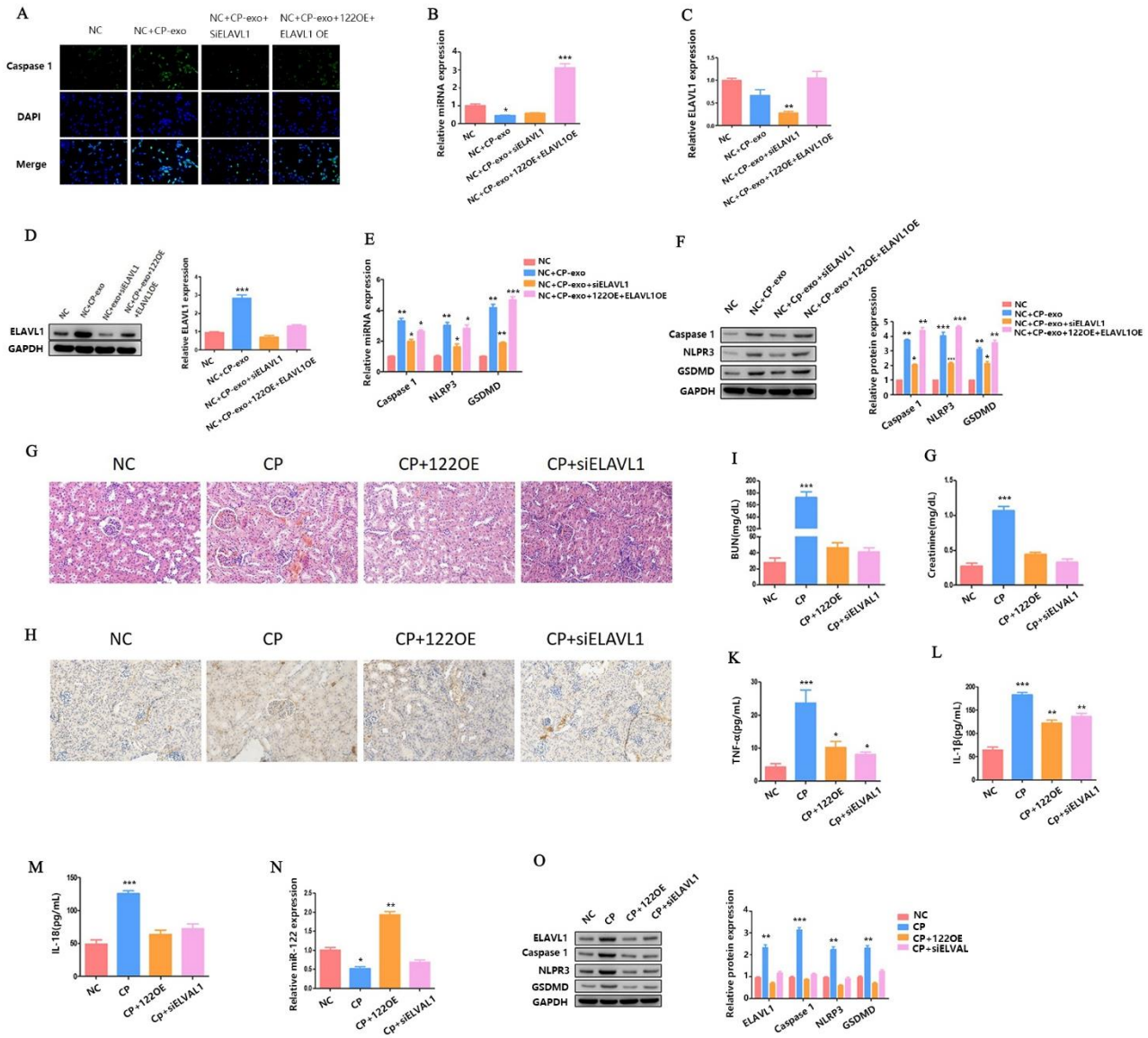

Fig. 4. Exosome-derived miR-122 affects cisplatin-induced AKI and HK2 cells pyroptosis by regulating the expression of ELAVL1. (**A**) IF staining shows expression of caspase-1 (green); Blue fluorescence represents the nucleus (DAPI). Bar, 100 mm. (**B-C**) The qPCR analysis of miR-122 and ELAVL1 expression. (**D**) WB analysis of ELAVL1 expression. (**E**) The qPCR analysis of caspase-1, NLRP3, and GSDMD expression. (**F**) WB analysis of caspase-1, NLRP3, and GSDMD expression. (**G**) H&E staining assays. (**H**) The distribution of GSDMD in kidney tissues as measured using IHC. (**I-M**) The blood from AKI mice is checked for BUN, serum creatinine, TNF-α, IL-1β, and IL-18 concentration. (**N**) The qPCR analysis of miR-122 expression. (**O**) The WB analysis of ELAVL1, caspase-1, NLRP3, and GSDMD expression. Data are shown as mean ± SEM (n = 3). Asterisks indicate significant differences from the control (*$P < 0.05$; **$P < 0.01$; ***$P < 0.001$).

Exosome-derived miR-122 affected cisplatin-induced AKI and HK2 cells pyroptosis by regulating the expression of ELAVL1.

In order to further explore the role of miR-122-ELAVL1 axis in pyroptosis regulation pathway under cisplatin-induced AKI, we first transfected the siELAVL1, miR-122 OE + ELAVL1 OE plasmid into the HK2 cell line. Then, we extracted the exosomes of these cell lines after cisplatin treatment. Exosomes derived from these cell lines were co-incubated with HK2 cells (NC) to detect the expression of caspase-1 via IF. As shown in Fig. 4A, the expression level of caspase-1 was significantly increased when cp-exo treatment was added. However, the expression level of caspase-1 was significantly decreased when cp-exo derived from siELAVL1 HK2 cell line treatment was added. In contrast, the expression level of caspase-1 was also significantly increased when cp-exo derived from miR-122 OE + ELAVL1 OE HK2 cell line treatment was added.

At the same time, we detected the expression of miR-122 and ELAVL1 using qRT-PCR or WB. The experimental results were consistent with the expected

results (Fig.4 B-D). Next, we also detected the mRNA and protein expression levels of caspase-1, NLRP3, and GSDMD using qRT-PCR and WB, respectively. As shown in Fig. 4E, the mRNA expression levels of caspase-1, NLRP3, and GSDMD were significantly increased when cp-exo treatment was added. However, the expression levels of caspase-1, NLRP3, and GSDMD were significantly decreased when cp-exo derived from siELAVL1 HK2 cell line treatment was added.

In contrast, the expression levels of caspase-1, NLRP3, and GSDMD were also significantly increased when cp-exo derived from miR-122 OE + ELAVL1 OE HK2 cell line treatment was added. The variation trend of caspase-1, NLRP3, and GSDMD protein expression was consistent with that of mRNA (Fig.4 F). Taken together, these results indicate that the miR-122-ELAVL1 axis involved in cisplatin-treated HK2 cell exosomes affected the surrounding HK2 cell pyroptosis.

Finally, we verified our hypothesis in vivo. We detected the extent of histopathological damage to the renal cortex of cisplatin-induced AKI mice using H&E staining when miR-122 was overexpressed (OE) or ELAVL1 was knocked down (KD). As shown in Fig. 4G, either overexpressing miR-122 or knocking down ELAVL1 alleviated cisplatin-induced AKI. We also detected the expression of GSDMD in kidney tissue using IHC analysis. As shown in Fig. 4H, the expression of GSDMD in the miR-122 OE and siELAVL1 AKI mice were all significantly decreased when compared with the model group.

In addition, the levels of blood urea nitrogen (BUN) (Fig. 4I), serum creatinine (Fig. 4J), TNF-α (Fig. 4K), Interleukin-1β (IL-1β) (Fig. 4L) and Interleukin-18 (IL-18) (Fig. 4M) were significantly decreased in the miR-122 OE and siELAVL1 AKI mice. We also checked the expression of miR-122 in the miR-122 OE and siELAVL1 AKI mice (Fig. 4N). At the same time, we detected the expression of ELAVL1, caspase-1, NLRP3, and GSDMD proteins in the miR-122 OE and siELAVL1 AKI mice. The results were in line with expectations (Fig. 4O). All in all, these results indicate that miR-122 inhibited cisplatin-induced AKI and HK2 cells pyroptosis via ELAVL1.

Discussion

Cisplatin is an effective chemotherapy drug and has been widely used to treat solid tumors. However, it usually causes AKI in these patients. It has been found in previous studies that renal insufficiency can independently predict poor prognosis in cancer patients [29]. However, to date, the mechanism of cisplatin-induced AKI has not been studied in depth, and there is still no effective treatment. The pathological features of AKI are renal tubular cell damage, inflammation, and vascular dysfunction. Among them, renal tubular cell death is a common histopathological feature of AKI, and it is generally considered to be one of the factors leading to impaired renal function [30].

Pyroptosis is a proinflammatory programmed cell death regulated by caspases, and its role in kidney damage has been gradually discovered in recent years [31]. There are reports of the role of pyroptosis of RTECs in cisplatin-induced AKI [12]. In this study, we also used cisplatin induction to construct AKI mouse models and detected the expression of GSDMD, caspase-1, and GSDMD-N, the key targets of pyroptosis using IHC and WB, respectively (Fig. 1A-G). Then we used the HK2 cell line for in vitro experiments. Through IF and WB, we found that cisplatin treatment of HK2 cells significantly increased the expression of caspase-1 and GSDMD-N, respectively (Fig. 1H-J). These results suggest that pyroptosis was involved in regulation of cisplatin-induced AKI. This finding is consistent with previous reports. However, the regulatory mechanism is not yet clear. Studying the molecular mechanism of RTECs pyroptosis in cisplatin-induced AKI has thus become an area of exploration for the development of new AKI therapies.

Exosomes act as an important medium of communication between cells. Exosomes participate in immune regulation, information transmission, and antigen presentation [32]. Substances encapsulated in exosomes, especially miRNAs, play a vital role in the pathogenesis of various kidney diseases [33]. Exosomes derived from human bone mesenchymal stem cells (hBMSCs) can prevent renal ischemia/reperfusion (I/R)injury through miR-199a-3p transplantation [34]. Exosome miRNA-19b-3p of RTECs promotes the activation of M1 macrophages during kidney injury [35]. However, there are a few studies on exosome miRNAs in cisplatin-induced AKI, and the mechanism is not clear.

In the present study, when we first added cisplatin and GW4869 to treat HK2 cells at the same time, we found that the phenomenon of pyroptosis was suppressed (Fig. 2A-D), which initially explained our hypothesis. Therefore, we further isolated and identified the exosomes of HK2 cells (Fig. 2E-G). Previous studies found that LncRNA XIST regulates the expression of ASF1A/BRWD1M/PFKFB2 through sponge adsorption

of miR-212 and thus participates in the regulation of acute renal injury in renal transplantation [36].

We measured the expression of miR-122 in AKI mice and HK2 cells when cisplatin treatment was added. As shown in Fig. 3A-B, when cisplatin was added, the expression of miR-122 was significantly downregulated. We further added GW4869 and found that the expression of miR-122 was significantly restored (Fig. 3C). To verify the role of miR-122 in cisplatin-induced pyroptosis of HK2 cells, we constructed miR-122 OE and miR-122 KD cell lines. Subsequently, we added cisplatin treatment to the miR-122 OE cell line, extracted the exosomes and incubated the exosomes with the HK2 cell line. We then tested the relevant indicators of pyroptosis. We also measured the relevant indicators of pyroptosis in miR-122 KD HK2 cell line. The results showed that miR-122 inhibited the effect of cisplatin-treated HK2 cell exosomes on the pyroptosis of surrounding HK2 cells (Fig. 3D-G).

Next, we identified ELAVL1 as a specific target for miR-122 to regulate pyroptosis in HK2 cells (Fig. 3I). Previous studies found that MALAT1 regulates renal tubular epithelial pyroptosis by modulated miR-23c targeting of ELAVL1 in diabetic nephropathy [37]. However, the role of ELAVL1 in cisplatin-induced AKI has not been reported. In the present study, we first clarified the relationship between miR-22 and ELAVL1 through the luciferase assay (Fig. 3J). Then, we detected ELAVL1 protein expression in cisplatin-treated mice and cells. The results showed that cisplatin treatment significantly increased the expression of ELAVL1 (Fig. 3K-L). We found that cisplatin-treated HK2 cell exosomes affected the surrounding HK2 pyroptosis (Fig. 3M-N). Finally, through a functional backfill experiment, we confirmed that miR-122 inhibited cisplatin-induced AKI and HK2 cells pyroptosis via ELAVL1 (Fig. 4).

In conclusion, to the best of our understanding, this study is the first to describe how miR-122 affects the pyroptosis of RTECs in cisplatin-induced AKI by regulating the expression of ELAVL1. This provides a new perspective for the treatment of AKI.

Preprint statements

This study was published in preprint on the following platforms: Bei Zhu, Xiaoshuang Ye, Fei Gao et al. Cisplatin induces acute kidney injury and pyroptosis in mice through the exosome miR-122/ELAVL1 regulatory axis, 16 July 2020, PREPRINT (Version 1) available at Research Square [https://doi.org/10.21203/rs.3.rs-41893/v1]

Conflict of Interest

There is no conflict of interest.

Acknowledgements

The work was supported by Elderly health project in Jiangsu Province (LKM2022001): Mechanism of bone marrow mesenchymal stem cell-derived microvesicles in ischemic kidney injury repair via miR-34a/Notch signaling pathway, and National Key Research and Development Program of China (2023YFC3605500).

We would like to thank all the researchers and study participants for their contributions.

References

1. Zhang W, Chen C, Jing R, Liu T, Liu B. Remote Ischemic Preconditioning Protects Cisplatin-Induced Acute Kidney Injury through the PTEN/AKT Signaling Pathway. Oxid Med Cell Longev. 2019;2019:7629396. https://doi.org/10.1155/2019/7629396
2. Pabla N, Dong Z. Cisplatin nephrotoxicity: mechanisms and renoprotective strategies. Kidney Int. 2008;73(9):994-1007. https://doi.org/10.1038/sj.ki.5002786
3. Dupre TV, Doll MA, Shah PP, et al. Suramin protects from cisplatin-induced acute kidney injury. Am J Physiol Renal Physiol. 2016;310(3):F248-F258. https://doi.org/10.1152/ajprenal.00433.2015
4. Crona DJ, Faso A, Nishijima TF, McGraw KA, Galsky MD, Milowsky MI. A Systematic review of strategies to prevent cisplatin-induced nephrotoxicity. oncologist. 2017;22(5):609-619. https://doi.org/10.1634/theoncologist.2016-0319
5. Holditch SJ, Brown CN, Lombardi AM, Nguyen KN, Edelstein CL. Recent Advances in Models, Mechanisms, Biomarkers, and Interventions in Cisplatin-Induced Acute Kidney Injury. Int J Mol Sci. 2019;20(12):3011. https://doi.org/10.3390/ijms20123011
6. Mulay SR, Linkermann A, Anders HJ. Necroinflammation in Kidney Disease. J Am Soc Nephrol. 2016;27(1):27-39. https://doi.org/10.1681/ASN.2015040405

7. Weijl NI, Elsendoorn TJ, Lentjes EG, et al. Supplementation with antioxidant micronutrients and chemotherapy-induced toxicity in cancer patients treated with cisplatin-based chemotherapy: a randomised, double-blind, placebo-controlled study. Eur J Cancer. 2004;40(11):1713-1723. https://doi.org/10.1016/j.ejca.2004.02.029
8. Yang C, Guo Y, Huang TS, et al. Asiatic acid protects against cisplatin-induced acute kidney injury via anti-apoptosis and anti-inflammation. Biomed Pharmacother. 2018;107:1354-1362. https://doi.org/10.1016/j.biopha.2018.08.126
9. Place DE, Kanneganti TD. Cell death-mediated cytokine release and its therapeutic implications. J Exp Med. 2019;216(7):1474-1486. https://doi.org/10.1084/jem.20181892
10. Martin SJ. Cell death and inflammation: the case for IL-1 family cytokines as the canonical DAMPs of the immune system. FEBS J. 2016;283(14):2599-2615. https://doi.org/10.1111/febs.13775
11. Zhang Z, Shao X, Jiang N, et al. Caspase-11-mediated tubular epithelial pyroptosis underlies contrast-induced acute kidney injury. Cell Death Dis. 2018;9(10):983. https://doi.org/10.1038/s41419-018-1023-x
12. Ye Z, Zhang L, Li R, et al. Caspase-11 Mediates Pyroptosis of Tubular Epithelial Cells and Septic Acute Kidney Injury. Kidney Blood Press Res. 2019;44(4):465-478. https://doi.org/10.1159/000499685
13. Wang Y, Zhang H, Chen Q, et al. TNF-α/HMGB1 inflammation signalling pathway regulates pyroptosis during liver failure and acute kidney injury. Cell Prolif. 2020;53(6):e12829. https://doi.org/10.1111/cpr.12829
14. Chen F, Lu J, Yang X, et al. Acetylbritannilactone attenuates contrast-induced acute kidney injury through its anti-pyroptosis effects. Biosci Rep. 2020;40(2):BSR20193253. https://doi.org/10.1042/BSR20193253
15. Miao N, Yin F, Xie H, et al. The cleavage of gasdermin D by caspase-11 promotes tubular epithelial cell pyroptosis and urinary IL-18 excretion in acute kidney injury. Kidney Int. 2019;96(5):1105-1120. https://doi.org/10.1016/j.kint.2019.04.035
16. Zhang J, Li S, Li L, et al. Exosome and exosomal microRNA: trafficking, sorting, and function. Genomics Proteomics Bioinformatics. 2015;13(1):17-24. https://doi.org/10.1016/j.gpb.2015.02.001
17. Qiu G, Zheng G, Ge M, et al. Mesenchymal stem cell-derived extracellular vesicles affect disease outcomes via transfer of microRNAs. Stem Cell Res Ther. 2018;9(1):320. https://doi.org/10.1186/s13287-018-1069-9
18. Gheinani AH, Vögeli M, Baumgartner U, et al. Improved isolation strategies to increase the yield and purity of human urinary exosomes for biomarker discovery. Sci Rep. 2018;8(1):3945. https://doi.org/10.1038/s41598-018-22142-x
19. Lv LL, Wu WJ, Feng Y, Li ZL, Tang TT, Liu BC. Therapeutic application of extracellular vesicles in kidney disease: promises and challenges. J Cell Mol Med. 2018;22(2):728-737. https://doi.org/10.1111/jcmm.13407
20. Guan H, Peng R, Mao L, Fang F, Xu B, Chen M. Injured tubular epithelial cells activate fibroblasts to promote kidney fibrosis through miR-150-containing exosomes. Exp Cell Res. 2020;392(2):112007. https://doi.org/10.1016/j.yexcr.2020.112007
21. Pan T, Jia P, Chen N, et al. Delayed Remote Ischemic Preconditioning ConfersRenoprotection against Septic Acute Kidney Injury via Exosomal miR-21. Theranostics. 2019;9(2):405-423. https://doi.org/10.7150/thno.29832
22. Meng XM, Ren GL, Gao L, et al. NADPH oxidase 4 promotes cisplatin-induced acute kidney injury via ROS-mediated programmed cell death and inflammation. Lab Invest. 2018;98(1):63-78. https://doi.org/10.1038/labinvest.2017.120
23. Zhang R, Yin L, Zhang B, et al. Resveratrol improves human umbilical cord-derived mesenchymal stem cells repair for cisplatin-induced acute kidney injury. Cell Death Dis. 2018;9(10):965. https://doi.org/10.1038/s41419-018-0959-1
24. Wu M, Wang Y, Yang D, et al. A PLK1 kinase inhibitor enhances the chemosensitivity of cisplatin by inducing pyroptosis in oesophageal squamous cell carcinoma [published correction appears in EBioMedicine. 2019 May;43:650] [published correction appears in EBioMedicine. 2021;63:103041]. EBioMedicine. 2019;41:244-255. https://doi.org/10.1016/j.ebiom.2019.02.012
25. Li ZL, Lv LL, Tang TT, et al. HIF-1α inducing exosomal microRNA-23a expression mediates the cross-talk between tubular epithelial cells and macrophages in tubulointerstitial inflammation. Kidney Int. 2019;95(2):388-404. https://doi.org/10.1016/j.kint.2018.09.013

26. Bao H, Zhang Q, Liu X, et al. Lithium targeting of AMPK protects against cisplatin-induced acute kidney injury by enhancing autophagy in renal proximal tubular epithelial cells. FASEB J. 2019;33(12):14370-14381. https://doi.org/10.1096/fj.201901712R
27. Ho J, Kreidberg JA. The long and short of microRNAs in the kidney. J Am Soc Nephrol. 2012;23(3):400-404. https://doi.org/10.1681/ASN.2011080797
28. Lee CG, Kim JG, Kim HJ, et al. Discovery of an integrative network of microRNAs and transcriptomics changes for acute kidney injury. Kidney Int. 2014;86(5):943-953. https://doi.org/10.1038/ki.2014.117
29. Yang Y, Li HY, Zhou Q, et al. Renal Function and All-Cause Mortality Risk Among Cancer Patients. Medicine (Baltimore). 2016;95(20):e3728. https://doi.org/10.1097/MD.0000000000003728
30. Linkermann A, Chen G, Dong G, Kunzendorf U, Krautwald S, Dong Z. Regulated cell death in AKI. J Am Soc Nephrol. 2014;25(12):2689-2701. https://doi.org/10.1681/ASN.2014030262
31. Tonnus W, Gembardt F, Latk M, et al. The clinical relevance of necroinflammation-highlighting the importance of acute kidney injury and the adrenal glands. Cell Death Differ. 2019;26(1):68-82. https://doi.org/10.1038/s41418-018-0193-5
32. Barile L, Vassalli G. Exosomes: Therapy delivery tools and biomarkers of diseases. Pharmacol Ther. 2017;174:63-78. https://doi.org/10.1016/j.pharmthera.2017.02.020
33. Zhang W, Zhou X, Zhang H, Yao Q, Liu Y, Dong Z. Extracellular vesicles in diagnosis and therapy of kidney diseases. Am J Physiol Renal Physiol. 2016;311(5):F844-F851. https://doi.org/10.1152/ajprenal.00429.2016
34. Zhu G, Pei L, Lin F, et al. Exosomes from human-bone-marrow-derived mesenchymal stem cells protect against renal ischemia/reperfusion injury via transferring miR-199a-3p. J Cell Physiol. 2019;234(12):23736-23749. https://doi.org/10.1002/jcp.28941
35. Lv LL, Feng Y, Wu M, et al. Exosomal miRNA-19b-3p of tubular epithelial cells promotes M1 macrophage activation in kidney injury. Cell Death Differ. 2020;27(1):210-226. https://doi.org/10.1038/s41418-019-0349-y
36. Cheng Q, Wang L. LncRNA XIST serves as a ceRNA to regulate the expression of ASF1A, BRWD1M, and PFKFB2 in kidney transplant acute kidney injury via sponging hsa-miR-212-3p and hsa-miR-122-5p. Cell Cycle. 2020;19(3):290-299. https://doi.org/10.1080/15384101.2019.1707454
37. Li X, Zeng L, Cao C, et al. Long noncoding RNA MALAT1 regulates renal tubular epithelial pyroptosis by modulated miR-23c targeting of ELAVL1 in diabetic nephropathy. Exp Cell Res. 2017;350(2):327-335. https://doi.org/10.1016/j.yexcr.2016.12.006